

Fifth Quarterly Progress Report

August 1, 2007 to October 31, 2007

Contract No. HHS-N-260-2006-00005-C

Neurophysiological Studies of Electrical Stimulation for the Vestibular Nerve

Submitted by:

James O. Phillips, Ph.D.^{1,3,4}

Steven Bierer, Ph.D.^{1,3,4}

Albert F. Fuchs, Ph.D.^{2,3,4}

Chris R.S. Kaneko, Ph.D.^{2,3}

Leo Ling, Ph.D.^{2,3}

Kaibao Nie, Ph.D.^{1,4}

Jay T. Rubinstein, M.D., Ph.D.^{1,4,5}

¹ Department of Otolaryngology-HNS, University of Washington, Seattle, Washington

² Department of Physiology and Biophysics, University of Washington, Seattle, Washington

³ Washington National Primate Research Center, University of Washington, Seattle, Washington

⁴ Virginia Merrill Bloedel Hearing Research Center, University of Washington, Seattle, Washington

⁵ Department of Bioengineering, University of Washington, Seattle, Washington

Reporting Period: May 1, 2007 – July 31, 2007

(1) Stimulation Device Development

In quarter 5 we received two fully functional sterile prototype UW/Cochlear primate vestibular implants. One of these has now been successfully implanted in a rhesus monkey, but this procedure occurred after the October 31st cut off for this report. In addition, we successfully implanted a vestibular nerve stimulation chamber and a vestibular nucleus recording chamber in a second animal, and initiated nerve mapping studies in that animal. We are mapping the nerve where it passes under the flocculus of the cerebellum using single unit tungsten microelectrodes advanced with a microdrive. After completion of the nerve mapping with recording and stimulation, we will implant a multiple single unit hybrid electrode (similar to our multiple single unit recording electrodes) in an optimal location to elicit VOR (vestibular-ocular reflex) behavior. We have received two fully functional prototype hybrid electrodes from NeuroNexus, which can be used for this purpose (see below). At that point, we will have both a proximal vestibular nerve stimulation electrode in one monkey and a distal end organ stimulation electrode (the UW/Cochlear primate vestibular implant) in a second monkey for our stimulation studies. We will compare and contrast the effects, on both eye movement behavior and the behavior of vestibular neurons, of parametric stimulation at these two sites.

(2) Software Interface Development

Spike detection and sorting

We have made improvements to the off-line spike detection and sorting algorithms in quarter 5. We have focused primarily on the identification and separation of overlapping waveforms. This analysis can be applied both to spike detection and to the disambiguation of overlapping neural activity and electrical stimulus artifact. For example, an overlap can occur when the action potentials from two neurons that are recorded on a single electrode occur within a short period of time (< 1 ms). Because the assignment of a spike to one neuron or the other is typically based on its temporal waveform, overlaps may result in some spikes being either misclassified or unclassified. The neurons that we are recording in this contract are especially vulnerable to overlap errors. Many vestibular and oculomotor neurons are characterized by high rates of spike discharge and the interval between two consecutive spikes carries important information related to head or eye movements. Thus, even a few unclassified or wrongly attributed spikes can adversely affect the analysis of the data. Furthermore, the use of closely spaced multi-channel recording arrays, in which the same spike can be detected on more than one channel, can potentially increase the frequency of overlap occurrences because a greater number of neurons are sampled simultaneously.

In figure 1 below, a trace displays a short segment of neural data recorded from the abducens nucleus of a rhesus monkey making gaze shifts to a visual target. The abducens, which is one target of the vestibular nuclei, contains the motoneurons of the

lateral rectus muscle. Two units are apparent in the trace. They are usually discriminable based on their different spike magnitudes. Characteristic of many neurons in this brain region, the units fire regularly, though at slightly different average rates. The tick marks above the data indicate where a candidate spike was detected, based on a simple voltage threshold crossing. Whenever the spike waveforms of the two units overlap, indicated by the black arrows, only one event is registered and the waveform of that event does not resemble either of the prototypical isolated spike waveforms. Thus, if the objective of the a spike detection and sorting routine is to correctly identify all spikes belonging to the large unit, discarding all occurrences of the small unit as noise, a significant overlap will cause an error because the shape of the compound waveform will not be recognized. Alternatively, if the objective is to identify the spikes of both units, then for more severe overlaps, the smaller spike will not even be detected as a distinct event.

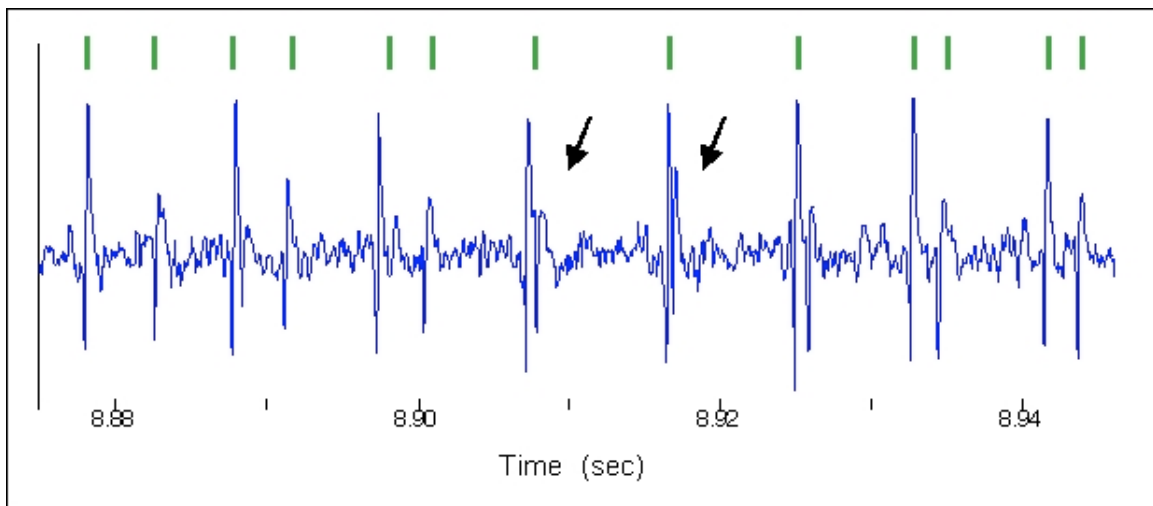


Figure 1. A train of extracellularly recorded action potentials in the abducens nucleus where two recorded units of differing amplitude overlap.

To address this problem, we developed programs to isolate occasionally overlapping spikes. The spike detection and sorting, including overlap resolution, was carried out in several steps. The algorithms, which are available on the project website, were implemented in the MATLAB programming environment. The examples given here are for a single recording channel, but the processing steps are being augmented to handle multi-channel data by creating templates across channels. The following steps are implemented in this process.

Event Detection: Detection was carried out by first applying a 2-point differentiation to the raw voltage signal to accentuate regions of fast change in the spike waveform. The resulting signal was squared and summed over a sliding 0.2 ms window. A threshold was then calculated as 2.2 times the standard deviation of the voltage values over the entire signal. Values greater than the threshold were accepted as events for further processing. The timing of each triggered event was aligned to the point of the most negative voltage deflection. A 0.8 ms lockout period was imposed after each event, to avoid double-counting spurious threshold crossings and to prevent triggering on a spike coming too

close in time to another spike. The lockout period improved the ability to resolve spike overlaps during the later processing step.

Event Extraction. For each detected event, a short clip of the voltage trace was stored. The extraction window covered 0.4 ms prior to and 1.0 ms after the trigger alignment.

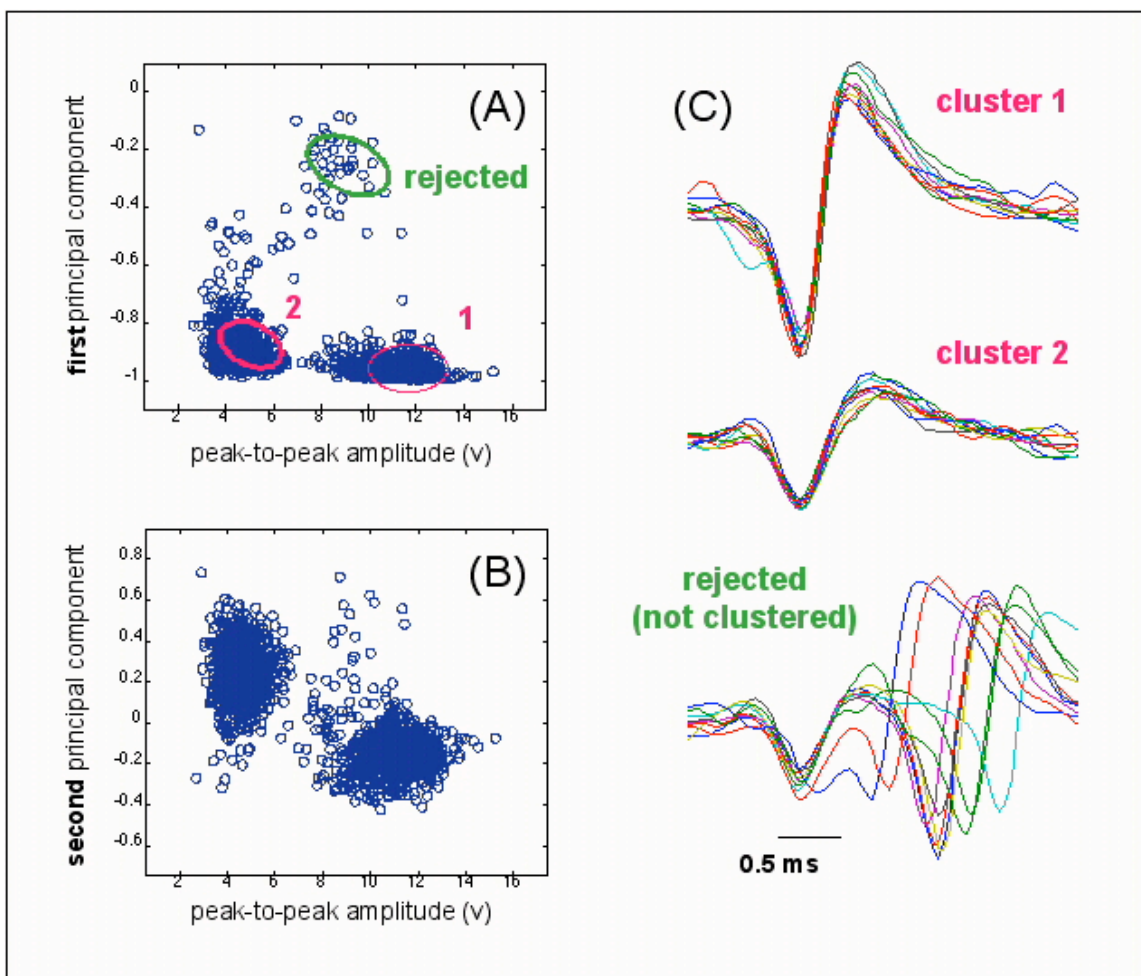


Figure 2. Parameter clustering. A parameter clustering approach is illustrated for the waveforms recorded in figure 1. The first principal component (A) and the second principal component (B) are plotted against peak to peak amplitude. This results in (C) separation of the component spikes and a group of ambiguous (rejected) waveforms

Parameter Clustering. The purpose of this step was to identify those event waveforms that are most representative of a particular neuron's spikes. We chose to use a manual clustering procedure, though an automatic procedure like the K-means algorithm has produced similar results. Three event waveform parameters were used for clustering; i.e., the peak-to-peak amplitude and the first and second principle components. During the procedure, the user was prompted to draw a box around a cluster formed in 2 dimensions from two of the three parameters (Figure 2 A). This brought up a separate MATLAB window showing the overlaid event waveforms. The user then indicated that the

selection was correct; i.e., waveforms were consistent in shape and fairly representative of the target neuron's spikes, containing little noise and no obvious overlaps. Then the next pair of parameters was displayed (Figure 2, B) but containing only the subset of events chosen in the first iteration. The clustering proceeded until all three pairs of parameters were clustered. Then another target neuron was chosen and the procedure was repeated. At any time the user can redraw the last set of boundaries.

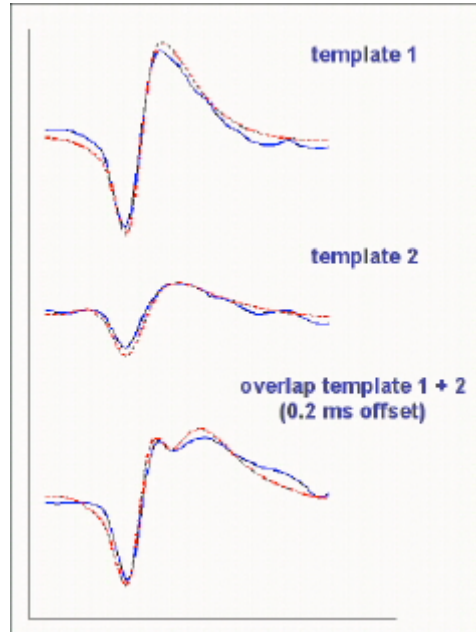


Figure 3. Templates formed from the analysis in figure 2. The upper two panels indicate the derived templates, while the lower panel indicates a template derived from the overlap of the templates above. The templates are indicated in red, while a typical waveform is indicated in blue.

Template formation. Spike templates for each neuron were constructed by averaging the clustered event waveforms of the previous step.

Spike sorting phase 1. Non-overlap template matching. The first phase of spike sorting was to compare all detected events (not just those manually clustered) to the single-unit spike templates. Time points from 0.2 ms before the peak alignment to 0.6 ms after alignment were used for this step. An event waveform was considered a match if two criteria were met: 1) the template gave a lower RMS error than any other template, and 2) no more than 5% of the points lay outside a tolerance range, defined as 2.0 times the average RMS error of the originally clustered events. Matching to a template was intentionally made stringent, to provide a high level of confidence for classifying spikes in this first phase. Examples of successfully matched event waveforms are given in Fig. 3.

Spike sorting phase 2: Overlap template matching. Typically, most candidate spikes were not classified during the first phase of template matching. For the second phase, a series of overlap templates were generated. These consisted of all permutations of two templates, with one template aligned as usual and the other occurring at a series of

negative and positive temporal offsets. The offsets ranged from 0.25 ms before the waveform peak to 0.75 ms after, in steps equal to the sampling period. The shifted and unshifted templates were added, employing zero-padding at the template ends when needed. Templates were never added to themselves, but a series of shift-only templates were constructed to allow for misalignment or false-triggering due to spurious peaks in the voltage signal; i.e., due to distant spiking neurons or local field potentials. Matching to the overlap and shift templates proceeded as in phase 1, but the level of tolerance was increased to 2.3 times the average RMS error and up to 7% of the points could lie outside of the tolerance range. An example of a successful match to an overlap template is shown in the bottom panel of Figure 3. Although the event waveform had an unusual shape, the overlap template produced a good match.

(3) On-line Control of Stimulation

The functionalities of the pulse train generator were continuously improved during Quarter 5 to facilitate the recording of single neurons during stimulation and the removal of stimulus artifact. We made many changes in the software interface to create a reliable, easily used, and safe pulse generator for the animal experiments. Previously, only a user-initiated mode was supported by the program. In this mode, a pulse train was delivered at a short interval after a user presses the “Go” button on the graphical user interface. In this quarter, a new trigger mode was added to the software, which allows for the generation of a pulse train in sync with an external trigger signal from the recording device to the programming pod. The software was restructured to accommodate the external trigger mode.

In addition, we worked to implement another trigger mode using a trigger signal from a standard parallel I/O port. This will allow the behavior of the monkey, for example fixation of a target spot, to trigger the stimulation. In this mode, the pulse train generator can take external input triggers and it can also output a series of digital pulses signaling the timing of each single biphasic pulse in a trial. The eye movement recording system has full control over the pulse train generator and precisely knows the timing of a stimulation pulse train. This will be critical because the behavioral control software can then extinguish the target spot with the initiation of the stimulation. As part of this implementation effort, we have tested Matlab toolboxes that can read digital I/O signals from a parallel port.

We have also explored the possibility of adding high-rate conditioners to stimulation pulse trains to mimic the stochastic neural firing pattern. We received a newly-developed research tool—CDI3.2 (Cochlear Device Interface) from Cochlear Ltd. The tool will allow us to simultaneously create stimulation pulse trains and high-rate conditioners. We spent time learning how to program the new research tool, and communicating with researchers in the Cochlear technology center at Belgium on the installation and debugging of the CDI tool.

(4) Multi-channel Recording Device Development

This quarter we received two fully functional custom axial electrodes from NeuroNexus Technologies to initiate recording and stimulation studies. We are still awaiting the arrival of our full complement of specially designed electrodes, however. The design of the two existing electrodes will allow us to record from and stimulate the vestibular nerve proximal to the brainstem at several sites identified through single unit mapping. This will then serve as the “proximal nerve prosthesis” in our first rhesus monkey. Our initial vestibular nucleus recording is being performed with single unit microelectrodes, but we will transition to multiple single unit (axial) recording electrodes when they become available in sufficient quantities.

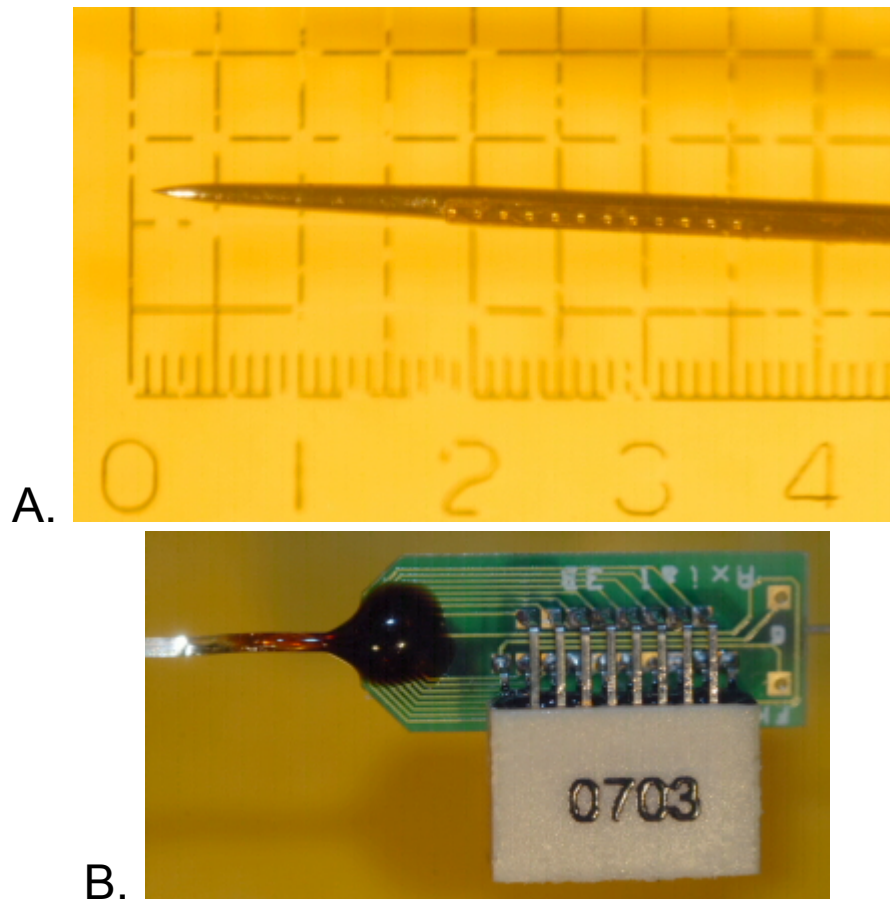


Figure 4. A working axial recording electrode. (A) The tip and axial recording sites of the electrode. (B) The connector end of the axial electrode

The current devices consist of a 180 micron diameter tungsten microelectrode covered by a thin-film substrate that carries 12 conducting leads. Each lead ends in an electrode contact, which are linearly spaced by 150 microns center-to-center. The 12 electrode sites are clearly seen figure 4A. The total length of the tungsten carrier is ~14 cm. 5 cm back from the tip, heat-shrink tubing (not shown in the figure) was added to support the carrier and protect the thin-film conducting leads. The tubing widens the diameter to about 280 microns, but this is still narrower than the metal cannula that is used to guide

the electrodes into the brain. At the back end of the device (Figure 4B), the leads are bonded to an 18-pin Omnetics connector, which attaches to our laboratory's multi-channel Plexon headstage.

(6) Dissemination of Information:

An important continuing objective of the contract is the dissemination of information to clinical and research groups locally. During the fifth quarter, we have continued our local presentations with a comprehensive presentation to the Clinical Vestibular Disorders Group, which meets monthly. Also, we have supplemented the information on our website.

(7) Overall Progress

We have now received fully functional versions of both the UW/Cochlear primate vestibular implant and the NeuroNexus Technologies axial electrodes. We have proceeded with implantation of a proximal nerve stimulation chamber (to utilize the axial electrode for proximal nerve stimulation) in one monkey and, recently, of a distal end-organ stimulation prosthesis in a second monkey. We have developed new software for stimulation and behavioral control, and analysis of recorded neural activity. We have purchased additional monkeys so that we will be able to complete a comparison study of the effects of stimulation at both sites in addition to fully accomplishing our other research objectives.

(8) Future Emphasis

We have a simple objective for our research activity in Quarter 6: to stimulate the vestibular nerve proximally in one animal, and distally in another animal, and compare the effect of stimulation at both sites. We anticipate that the UW Cochlear distal prosthesis will provide the best isolation of individual canal afferents, but it will require much higher current thresholds for activation of the nerve and to elicit behavior than the proximal stimulation electrode. There is a high probability that we will accomplish our Quarter 6 objectives because:

a. We currently have a working end organ stimulation device. We know this because we tested the impedances of UW Cochlear distal prosthesis immediately following implantation with the standard clinical test protocol for cochlear implants. The device had impedances on the order of 15 – 20 K Ohm per channel on all channels.

b. We have a successful surgical strategy and healthy research subject animals. Both animals are currently healthy and the implants are intact. Indeed, the animal that was implanted with the UW Cochlear distal prosthesis, showed very little nystagmus or postural instability immediately following the surgery, and resumed normal activities the following day. As part of our study, and to provide optimal animal care, we have implemented a regular monitoring protocol that will document the overall behavior of both animals outside of the test sessions as the study proceeds.

In addition to our stimulation studies, we will continue to improve the spike detection/sorting algorithms in the upcoming quarter. As we collect multi-channel data, and sort spikes based on their temporal and spatial waveform shapes, we will apply the spike sorting methods to an expanded parameter space. We will also track changes in template shapes over time. Finally, we will apply the overlap template method to the removal of electrical artifacts.